

Depth-dependent trophic strategies of Caribbean sponges on mesophotic coral reefs

Keir J. Macartney^{1,3,*}, M. Sabrina Pankey¹, Amelia Clayshulte Abraham², Marc Slattery², Michael P. Lesser¹

¹Department of Molecular, Cellular and Biomedical Sciences and School of Marine Science and Ocean Engineering, University of New Hampshire, Durham, NH 03824, USA

ABSTRACT: Mesophotic coral reef ecosystems (MCEs) are characterized by gradients in irradiance, temperature and trophic resources. As depth increases on Caribbean mesophotic reefs, particulate organic matter increases while dissolved organic matter decreases, and the increase in particulate organic matter is directly related to the increase in sponge abundances and growth rates on MCEs. To further understand the trophic ecology of sponges, changes in microbiome composition and function, stable isotopic composition and proximate biochemical composition of 4 Caribbean reef sponges (*Amphimedon compressa*, *Agelas tubulata*, *Plakortis angulospiculatus* and *Xestospongia muta*) were quantified along a shallow to mesophotic depth gradient on Grand Cayman Island. Increases in δ^{15} N for all sponges were observed as depth increased, indicating an increasing reliance on heterotrophic food resources. Species-specific changes in symbiotic microbial community composition were also observed as depth increased, and the predicted functional genes associated with nitrogen and carbon cycling showed species-specific changes between depths. Regardless of species-specific changes in microbiome community structure or function, or whether sponges were classified as high microbial or low microbial abundance, sponges increased their consumption of particulate organic matter with increasing depth into the lower mesophotic zone.

KEY WORDS: Sponges \cdot Coral reef \cdot Mesophotic \cdot Trophic ecology \cdot Microbiome \cdot Stable isotopes \cdot Carbon \cdot Nitrogen \cdot Particulate organic matter \cdot Dissolved organic matter

- Resale or republication not permitted without written consent of the publisher

1. INTRODUCTION

In the Caribbean, sponges are common members of coral reef ecosystems (Wulff 2012), and their roles in nutrient cycling and as essential habitat for numerous diverse and ecologically important reef species are well established (Diaz & Rützler 2001, Bell 2008, Fiore et al. 2010, de Goeij et al. 2013, 2017). Like many benthic marine species, sponges develop species-specific symbioses with microbial communities (i.e. microbiome) that can play many important roles in nutrient cycling *in hospite* and on coral reefs (Thacker & Freeman 2012, Fiore et al. 2013a,b, 2020, Bourne et al.

2016, Morrow et al. 2016, Pita et al. 2018). Sponge-associated microbes account for 35–50% of the total biomass of a sponge (Hentschel et al. 2006, Thomas et al. 2016) and have been shown to provide inorganic and organic resources to their host through chemosynthesis, photosynthesis and/or heterotrophy (Freeman & Thacker 2011, Fiore et al. 2013a, 2015, Rubin-Blum et al. 2019, Zhang et al. 2019, Rix et al. 2020). Sponges have co-evolved two different character states of symbiont association based on the relative density of microbes within the tissues of the host sponge (Pankey et al. 2022). High microbial abundance sponges (HMA) harbor 10⁸ to 10⁹ bacteria g⁻¹ of

²Department of BioMolecular Sciences, Division of Environmental Toxicology, University of Mississippi, Oxford, MS 38677, USA

³Present address: School of Earth, Environmental and Marine Sciences, University of Texas Rio Grande Valley, Port Isabel, TX 78958, USA

sponge tissue while low microbial abundance sponges (LMA) harbor 10⁵ to 10⁶ bacteria g⁻¹ of sponge tissue (Weisz et al. 2008, Hentschel et al. 2012, Gloeckner et al. 2014, Pita et al. 2018). For most sponges, their HMA or LMA status influences their trophic ecology. Early studies suggested that HMA sponges were unable to filter sufficient particulate organic matter (POM) from the surrounding seawater to support their energetic requirements. Therefore, HMA sponges were thought to supplement that resource with dissolved organic matter (DOM), whereas LMA sponges appeared to meet their energetic requirements using POM alone (Reiswig 1981, Weisz et al. 2008). Subsequent studies have shown that the trophic ecology of HMA versus LMA sponges is more nuanced (de Goeij et al. 2017) and that DOM uptake and assimilation can also be dependent on the sources of DOM (Rix et al. 2017).

Sponge-associated microbes significantly influence both the chemical and trophic ecology of the sponge, which in turn affects sponge depth distributions (e.g. Slattery et al. 2016) from shallow (<30 m) to mesophotic (~30-150 m) depths (Lesser et al. 2018). Specifically, sponges increase in abundance and percent cover with increasing depth into mesophotic coral reef ecosystems (MCEs) (Lesser et al. 2009, 2018, Garcia-Sais 2010, Lesser & Slattery 2018, Macartney et al. 2020, 2021a,b). MCEs have received increasing attention due to their potential role as refuges for threatened shallow reef species (Bongaerts et al. 2010, Slattery et al. 2011, Loya et al. 2016, Lesser et al. 2018; but see Bongaerts et al. 2017) and are characterized by gradients of abiotic factors such as decreasing photosynthetically active radiation (PAR; Lesser et al. 2009, 2018, 2021). In the Caribbean, many MCEs also show repeatable patterns in trophic resource availability, including increases in POM and concurrent decreases in DOM as depth increases (Lesser 2006, Trussell et al. 2006, Lesser & Slattery 2013, Lesser et al. 2019, 2020).

Biotic and abiotic factors that influence sponge distributions in the Caribbean have been studied extensively (Lesser 2006, Trussell et al. 2006, Pawlik et al. 2013, 2015, Lesser & Slattery 2018, Lesser et al. 2018, 2019), and while top-down control (i.e. predation) can affect sponge distributions, particularly within mangroves (e.g. Wulff 2017), bottom-up control is the primary factor affecting sponge distributions between shallow coral reefs and MCEs. Bottom-up forcing based on the increased availability and consumption of both DOM and POM significantly influences the ecological distributions and abundances of sponges from shallow to MCE depths (Lesser 2006, Trussell et

al. 2006, Lesser & Slattery 2013, 2018, Slattery & Lesser 2015, Lesser et al. 2019, 2020, Macartney et al. 2021a,b). Sponges increase their consumption of both POM and DOM as depth increases (Lesser 2006, Macartney et al. 2021b), and while POM is essential for sponge growth through the provision of nitrogen (Ducklow et al. 1993, Campbell et al. 1994, Lesser 2006), the DOM component of sponge diets is a major source of carbon for sponges, comprising up to 95 % of their carbon uptake (de Goeij et al. 2013, 2017, Mueller et al. 2014, McMurray et al. 2018, Wooster et al. 2019). While recent studies have clearly shown that sponge cells (i.e. choanocytes) can take up DOM, this resource is also consumed by the microbiome of the sponge, with rates dependent on whether it is an HMA or LMA sponge (Rix et al. 2020, Hudspith et al. 2021, Olinger et al. 2021). Reprocessed DOM, in the form of dissolved free amino acids, can also be translocated to the sponge host from the microbiome, as shown using compound-specific isotopic analysis of essential amino acids (Shih et al. 2020, Macartney et al. 2021a), or used to synthesize compounds for chemical defense (Olinger et al. 2021). While the proportion of organic material that is transferred from the microbiome to the sponge host has not been quantified (Rix et al. 2020), it should be noted that transfer of DOM-derived carbon and nitrogen from host cells to the microbiome has been observed (Rix et al. 2020), and direct phagocytosis of bacterial symbionts by host cells also occurs (Leys et al. 2018). While the microbiome of sponges has been described as stable over large temporal and spatial scales, environmental gradients can change the community composition of the sponge microbiome, and the magnitude of this change can be site-dependent (Morrow et al. 2016, Pita et al. 2018). Studies from the Caribbean and the Pacific have shown that changes in depth can affect the community composition of sponge microbiomes, driven by both abiotic and biotic factors (Olson & Gao 2013, Morrow et al. 2016, Steinert et al. 2016).

Here, a natural experiment (sensu Diamond 1986) on 3 HMA sponges (*Agelas tubulata, Plakortis angulospiculatus* and *Xestospongia muta*) and one LMA sponge (*Amphimedon compressa*) was conducted along a shallow to mesophotic depth gradient on Grand Cayman Island, where sponges increase in abundance with increasing depth as documented for several locations in the Caribbean basin (Lesser & Slattery 2018, Macartney et al. 2021a). We quantified the trophic strategies of these sponges and determined which species or symbiotic state (i.e. HMA vs. LMA) relies more heavily on POM or DOM as depth increases, using stable isotopes of carbon (δ^{13} C) and

nitrogen ($\delta^{15}N$) as trophic markers. Specifically, do changes in the biodiversity of the sponge microbiome occur as a function of depth into mesophotic habitats? Are changes in biodiversity associated with changes in trophic resource availability? And does heterotrophic uptake of DOM and POM change with the concentrations of these trophic resources, and is that reflected in their stable isotopic signatures, energetic reserves, community structure of their microbiomes and predicted metabolic profiles and relative functional capacity? These sponges represent a variety of morphologies (see Abraham et al. 2021), microbial associations (i.e. LMA vs. HMA) and trophic strategies, such as symbiosis with known photoautotrophic symbionts in X. muta (Morrow et al. 2016), compared to sponges that have low relative abundances of photoautotrophic symbionts such as A. tubulata (Gantt et al. 2019). Unlike studies on a single species, using multiple species of varying ecological phenotypes over gradients of abiotic factors should provide significant insight into the trophic ecology of these sponges.

2. MATERIALS AND METHODS

2.1. Study site

All environmental data and sponge samples were collected at the Kittiwake Anchor Buoy site, Grand Cayman (19.36° N, 81.40° W). This site exhibits a spur and groove morphology, with a sloping reef structure between 15-60 m, at which point the reef topography turns into a vertical wall. As depth increases into the mesophotic zone at this site, concentrations of particulate organic carbon and particulate organic nitrogen increase significantly, while dissolved organic carbon (DOC) and dissolved organic nitrogen (DON) decrease significantly (Lesser et al. 2018, 2019, Macartney et al. 2021b). Dissolved inorganic nitrogen as NO_x (i.e. $NO_3^- + NO_2^-$) increases significantly with depth at this site (Macartney et al. 2021b). Downwelling irradiance ($E_{\rm d}$), measured as PAR (400-700 nm), also exhibits a significant decrease as depth increases into the mesophotic zone (Lesser et al. 2018, 2021, Macartney et al. 2021b).

2.2. Sample collection

Samples of sponge tissue, ambient seawater and sediment porewater were collected at the study site. Tissue samples from individual sponges (i.e. genets) of *Agelas tubulata*, *Amphimedon compressa*, *Plakor*-

tis angulospiculatus and Xestospongia muta were collected along a depth gradient at 15, 22, 30, 46, 61, 76 and 91 m. Samples of A. tubulata, A. compressa and P. angulospiculatus were collected (n = 3-6 for each depth) at 15, 22, 30, 46 and 61 m, while X. muta was collected (n = 5-8 for each depth) at 15, 30, 61, 76 and 91 m. A. tubulata, P. angulospiculatus and X. muta were sampled by cutting a 'pie-slice' of sponge tissue from the apical lip of the osculum, including both pinacoderm and mesohyl, as described in Morrow et al. (2016); these tissues were placed in labeled bags filled with seawater. A. compressa was sampled as whole 'branches' and placed into labeled bags filled with seawater. For all species, sponge tissue was left at the base for regrowth after sampling. All sponges were kept in a shaded cooler, submerged in seawater, until transported to shore for sample processing. A small subsample was taken using a sterile razor and stored in DNA preservation buffer (Seutin et al. 1991) for subsequent 16S rRNA amplicon sequencing. Additional subsamples of tissue were collected for stable isotope analyses and immediately frozen at -20°C for transport to the University of New Hampshire (UNH), where they were frozen at -80°C until analysis. The remaining sponge tissue was frozen at -20°C and transported frozen to the University of Mississippi, where they were freeze-dried for proximate biochemical analyses.

Seawater samples were also taken at the surface and at 22, 30, 46, 61, 76 and 91 m (n = 3 per depth). Acid-washed 180 ml syringes were used to take samples approximately 1 m above the benthos at each depth, taking care to avoid any benthic organisms or sediment. Water samples were then filtered through a 0.2 µm baked GF/F filter that was stored in DNA buffer. Porewater was collected at 15 m (n = 3) by filling a 50 ml falcon tube half with sediment and half with seawater. These samples were then taken to the laboratory, mixed by inversion and allowed to settle, and samples of the supernatant were filtered as described above for seawater samples. Seawater and porewater DNA samples were immediately frozen at -20°C and transported frozen to UNH, where they were frozen at -80°C until analysis.

2.3. DNA isolation and 16S rRNA amplicon sequencing

To obtain genomic DNA, approximately 200–300 mg of sponge tissue was taken from a subsample stored in DNA buffer and blotted to remove any excess; the tissue was then cut into small pieces using a

sterile razor. Sponge DNA was isolated using a Qiagen DNeasy PowerSoil® extraction kit with a modified protocol as follows. Tissue was added to the PowerSoil bead tubes with 5 µl of Proteinase K (20 mg ml⁻¹ stock in 10% sodium dodecyl sulphate) and 2 µl of RNAse (Qiagen) before incubation at 55°C for 18 h. After this incubation, PowerSoil Kit Solution 1 was added, and samples subsequently underwent a bead-beating step using a Qiagen Tissue Lyser for 5 min at 50 Hz. The Qiagen DNeasy PowerSoil kit standard instructions were followed post bead-beating.

Microbial DNA was amplified using PCR, with primers targeting the universal prokaryotic 16S rRNA gene (sensu Lesser et al. 2020, Macartney et al. 2020). The forward primer 515F (5'-GTG YCA GCM GCC GCG GTA A-3'; Parada et al. 2016) and the reverse primer 806R (5'-GGA CTA CHV GGG TWT CTA AT-3'; Apprill et al. 2015) were used. Fluidigm linker sequences CS1 (5'-ACA CTG ACG ACA TGG TTC- TAC A-3') and CS2 (5'-TAC GGT AGC AGA GAC TTG GTC T-3') were then added to the 5' end of forward and reverse primers to facilitate next-generation sequencing. The 16S rRNA gene PCR consisted of a 25 µl reaction with 12.5 µl AmpliTag Gold 360 Master Mix (Applied Biosystems), 1.0 µl GCenhancer, 0.5 μ l 515F (10 μ M) and 0.5 μ l 806R $(10 \mu M)$, 2.0 µl of DNA template (20-30 ng) and 8.5 µl nuclease-free water (Integrated DNA Technologies). Reactions were performed using the following PCR protocol: initial denaturation for 10 min at 95°C, 30 cycles of 95°C for 45 s, 50°C for 60 s and 72°C for 90 s, followed by a 10 min extension at 72°C. Successful PCR reactions were confirmed by visualizing products on a 1% agarose gel. The PCR amplicons containing Fluidigm linkers were sequenced on an Illumina MiniSeq System employing V2 chemistry (2 × 150 bp reads) at the University of Illinois at Chicago Research Resources Center's Sequencing Core. Amplicon sequence variants (ASVs) were inferred and tabulated across samples using 'DADA2' (Callahan et al. 2016) utilizing established bioinformatic pipelines (Lesser et al. 2020, Macartney et al. 2020).

The analyses of sponge microbial communities were accomplished utilizing the R package 'phyloseq' (Mc-Murdie & Holmes 2015) in R (sensu Lesser et al. 2020). Samples with fewer than 10 000 counts were filtered from the ASV count table, and ASVs detected in more than 2 samples and at least 10 occurrences across samples were retained during the filtering process. Samples were then rarefied to account for sampling effort. To measure the alpha diversity for each sample, the Shannon diversity index was used. Ordination plots were produced based on Bray-Curtis

distance matrices using nonmetric multidimensional scaling (NMDS) (stress value: <0.0001). To assess compositional differences at varying taxonomic scales, the rarefied ASV count table was consolidated by rank using the phyloseq 'tax_glom' function and then raw counts were transformed to center log rations using the 'transform' function (CLR) from the R package 'microbiome' (Callahan et al. 2016). Microbial phylum and class compositional differences between depths for each sponge species were tested using permutational multivariate analysis of variance (PERMANOVA) in the R package 'vegan'. Any differences observed during post hoc testing at the class level for taxa between depths were tested using ANOVA and Tukey's HSD on dominant taxa (>1% reads). Phylum and class level were used for these analyses due to limitations in the (SILVA) database typically hindering classification beyond class level for the majority of ASVs, which is unsurprising given the novel diversity found in sponge microbiomes.

Predicted community profiles and functional capacities were assessed using PICRUSt2 (v.2.1.0-b), which uses the metagenomic data from available genomic databases (Langille et al. 2013, Langille 2018). The 16S rRNA ASVs were aligned with 'HMMER' (Eddy 2008) and then put in a reference tree provided by PICRUSt2 using 'EPA-ng' and 'GAPPA' (Barbera et al. 2019). Gene family copy numbers were predicted for 16S rRNA as well as the Kyto Encyclopedia of Genes and Genomes (KEGG) functions using the Enzyme Commission (EC) and KEGG Orthology (KO) accessions using hidden state prediction ('castor') based on ASV abundances and phylogenetic proximity to reference taxa with available genomes. To minimize error in gene content prediction due to poor matches to available genomes, any ASVs receiving nearest-sequenced-taxon-index (NSTI) scores below 2 were removed. The relative abundances of metabolic pathways encoded by each sponge's microbiome were predicted using MinPath (Ye & Doak 2009). Then the relative abundances of functional genes of interest (Table S1 in the Supplement at www.int-res.com/ articles/suppl/m693p125_supp.pdf) for sponges over the depth range sampled were assessed using linear regression on the relative abundances normalized to the total reads in the sample.

2.4. Stable isotope analyses

Subsamples of sponge tissue were collected using a sterile razor and dried at 55°C for 24 h before pulverizing into a powder. Samples were sent to the Marine

Biological Laboratory (Woods Hole, MA) for the analysis of bulk C and N, as well as the natural abundance of the stable isotopes $\delta^{15}N$ and $\delta^{13}C$. Prior to analysis, samples were acidified using 1 M HCL. No significant differences in $\delta^{15}N$ due to acidification were observed (Macartney et al. 2020, Schubert & Nielsen 2000) when using paired samples of acidified and nonacidified tissues. Samples were analyzed using a Europa ANCA-SL elemental analyzer-gas chromatograph attached to a continuous-flow Europa 20-20 gas source stable isotope ratio mass spectrometer. Carbon isotope results are reported relative to Vienna Pee Dee Belemnite, and nitrogen isotope results are reported relative to atmospheric air; both are expressed using delta (δ) notation in units per mil (%). The analytical precision of the instrument was $\pm 0.1\%$, and the mean precision of sample replicates was $\pm 0.4\%$ for δ^{13} C and $\pm 0.2\%$ for δ^{15} N.

2.5. Proximate biochemical composition

Samples for proximate biochemical composition (PBC) were freeze-dried and pulverized, and dry sample mass was recorded before the analysis of PBC. See Abraham et al. (2021) for details; but briefly, carbohydrates were extracted and quantified using the phenol-sulfuric acid method in microplate format described in Masuko et al. (2005). A standard curve was derived from glucose standards and used to calculate the concentration of carbohydrates in samples. Soluble protein was extracted and quantified using the Bradford method (Bradford 1976). A standard curve was derived from bovine serum albumin (BSA) standards and used to calculate the concentration of protein in samples. Lipids were extracted and quantified using a modified version of the gravimetric protocol described by Freeman et al. (1957), and inorganic tissue constituents (i.e. ash) were quantified using tissue placed in a pre-weighed aluminum foil weigh-boat that was baked at 500°C in a muffle furnace for 5 h as described by McClintock et al. (1991). All components of the PBC were normalized to ash-free dry weight as described in Abraham et al. (2021) and converted to energetic equivalents using the enthalpies of combustion for protein, carbohydrates and lipids as described by Gnaiger & Bitterlich (1984).

2.6. Statistical analyses

All statistical analyses were completed in either JMP (v.14) or R (v.3.6.2). The effects of depth and spe-

cies on the microbial community were assessed with PERMANOVA and ANOVA as described above. Multiple comparison post hoc tests (i.e. Tukey's HSD) were applied where appropriate. The effects of depth and species on stable isotope ratios and PBC were assessed using linear regression, with depth treated as a continuous variable. Trophic niche separation was assessed using the stable isotope values for each sponge in the program Stable Isotope Bayesian Ellipses in R (SIBER; Jackson et al. 2011). Niche position and overlap were determined using calculations described in Layman et al. (2007) and statistically tested using Hotelling's t-tests sensu Turner et al. (2010). Any variables not meeting the assumptions of normality were log transformed before analysis and back transformed for presentation.

3. RESULTS

3.1. 16S rRNA amplicon sequencing

A total of 5908 265 16S rRNA MiniSeq read-pairs were initially recovered from sequencing of the 4 sponge species, seawater and sediment porewater. After merging and quality-trimming with DADA2, 5572 585 read-pairs remained. These ranged from 67833 to 11001 with a mean of 31483 \pm 7860 reads per sample. A total of 8507 unique ASVs were initially recovered, but ASVs unique to 2 or less samples or with fewer than 10 total observations were removed from the data set, resulting in a total of 3709 unique ASVs for downstream analyses.

There were significant differences in mean Shannonalpha diversity between sponge species, seawater and sediment porewater (ANOVA: $F_{5,125} = 192.63$, p < 0.0001) (Fig. S1), with all species and water types significantly different from each other with the exception of Xestospongia muta and the filtered seawater samples (Tukey's HSD < 0.05) (Fig. S1). Between sponge species, X. muta had the highest mean (\pm SE) Shannon-alpha diversity (4.73 \pm 0.07), followed by Plakortis angulospiculatus (4.15 \pm 0.05) and Agelas tubulata (3.17 \pm 0.04), while Amphimedon compressa displayed the lowest mean Shannon-alpha diversity (2.66 ± 0.06) . There was no significant effect of depth on Shannon-alpha diversity for A. compressa (ANOVA: $F_{4,22}$ = 0.52, p = 0.71; Fig. S2A), A. tubulata (ANOVA: $F_{5.30} = 0.71$, p = 0.623; Fig. S2B) or *P. angulospiculatus* (ANOVA: $F_{4,22} = 1.77$, p = 0.17; Fig. S2C). However, there was a significant effect of depth on Shannon-alpha diversity for X. muta (ANOVA: $F_{4,25} = 3.81$, p = 0.017), with significant differences between sponges

at 76 and 15 m, which were significantly different from sponges from all other depths (Tukey's HSD < 0.05; Fig. S2D).

NMDS analysis of the beta diversity index, using Bray-Curtis distance matrices, showed significant differences in microbial community ASV composition between sponge species and sample type (PERM-ANOVA: $F_{5,125} = 44.68$, p = 0.001; Fig. 1). Three of the 4 sponges showed significant differences in ASV composition between depths. In the LMA sponge A. compressa, both the phyletic composition (PERM-ANOVA: $F_{4,22} = 1.93$, p = 0.048) and class composition (PERMANOVA: $F_{4,22} = 1.90$, p = 0.009) of the microbiome were significantly different between depths (Fig. 2A). This difference was driven by an increase in Class Nitrososphaeria within the Phylum Thaumarchaeota at 61 m, a decrease in Class Bacteroidia at 46 m relative to 15 m and decreases in Class Planctomycetacia in Phylum Planctomyctes from its maximum at 15 m (Tukey's HSD < 0.05) (Table S2). No significant differences were observed between depths in phyletic composition (PERMANOVA: $F_{4,30} = 0.96$,

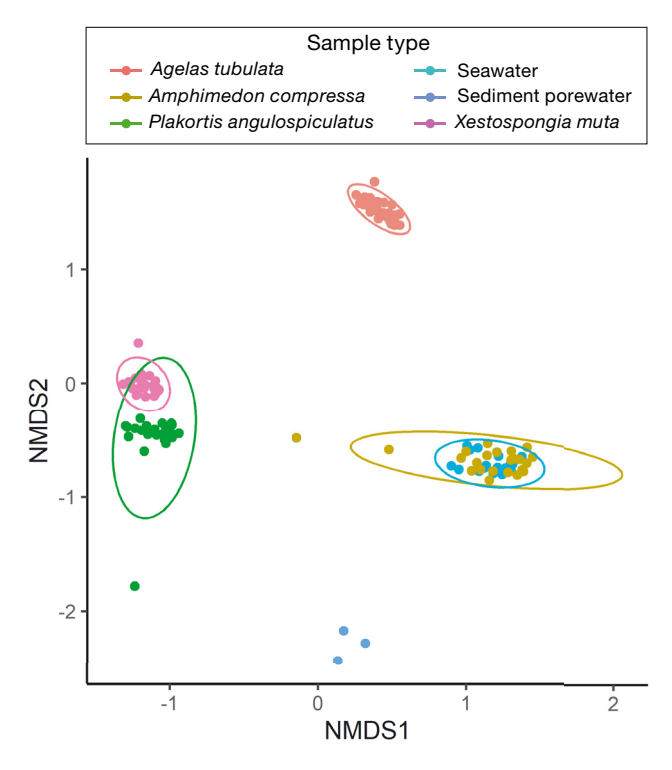


Fig. 1. Multidimensional analysis of β -diversity estimates using Bray-Curtis distance matrices of amplicon sequence variant composition for Amphimedon compressa, Agelas tubulata, Plakortis angulospiculatus, Xestospongia muta, sediment porewater and seawater microbial community composition. The 95% confidence interval ellipses are drawn to show species or sample type groupings

p = 0.511) or class-level composition (PERMANOVA: $F_{4,30} = 1.08$, p = 0.31) in the microbiome of *A. tubulata* (Fig. 2B).

For the microbiome of *P. angulospiculatus*, there was no significant differences between depths in phyletic composition (PERMANOVA: $F_{4,25}$ = 1.93, p = 0.234) but there was a significant effect of depth on class-level composition (PERMANOVA: $F_{4,25} = 1.56$, p = 0.006) (Fig. 2C). Post hoc testing showed that the Class Nitrososphaeria within Phylum Thaumarchaeota increased as depth increased to 61 m (Tukey's HSD < 0.05) (Table S2). There were significant decreases in classes Entotheonellia (Phylum Entotheonellaeota) and Acidobacteriia (Phylum Acidobacteria) at 46 m relative to all other depths, while Class Alphaproteobacteria (Phylum Proteobacteria) decreased at 46 m relative to all other depths (Tukey's HSD < 0.05) (Table S2). Class Spirochaetia (Phylum Spirochaetes) showed a significant increase between 30 and 46 m, but all other depths showed no significant differences (Tukey's HSD < 0.05). Class 'P9X2b3D02' in Phylum Nitrospinae significantly decreased at 61 m compared to 15 and 46 m, and the highest abundance was observed at 46 m (Tukey's HSD < 0.05; Fig. 2C). Class Deinococci in Phylum Deinoccoccus-Thermus showed significant increases as depth increased (Tukey's HSD < 0.05; Fig. 2C, Table S2).

For *X. muta*, both phylum- and class-level composition of the microbiome were significantly affected by depth (PERMANOVAs: $F_{4,25} = 2.98$, p = 0.001 and $F_{4.25}$ = 2.22, p = 0.001, respectively; Fig. 2D). Post hoc testing showed that Class 'TK17' in Phylum Chloroflexi decreased in abundance at 91 m while no other depths were significantly different from each other (Tukey's HSD < 0.05; Table S2). Class Anaerolineae in the Chloroflexi were significantly less abundant at 30 and 76 m relative to other depths (Tukey's HSD < 0.05; Table S2). Class Thermoanaerobaculia (Phylum Acidobacteria) and the Alphaproteobacteria (Phylum Proteobacteria) decreased as depth increased (Tukey's HSD < 0.05; Table S2). Class Rhodothermia (Phylum Bacteriodites) showed significant decreases in abundance after 30 m (Tukey's HSD < 0.05; Table S2). Class Nitrospira (Phylum Nitrospirae), Class 'Sub Group 6' of the Acidobacteria and Class Deinococci (Phylum Deinoccocus) were significantly higher in abundance at 91 m (Tukey's HSD < 0.05; Table S2) relative to other depths. Generally, Entotheonellia (Phylum Entotheonellaeota) and Spirochaetia (Phylum Spirochaetes) showed significant increases in abundance as depth increased (Tukey's HSD < 0.05; Table S2).

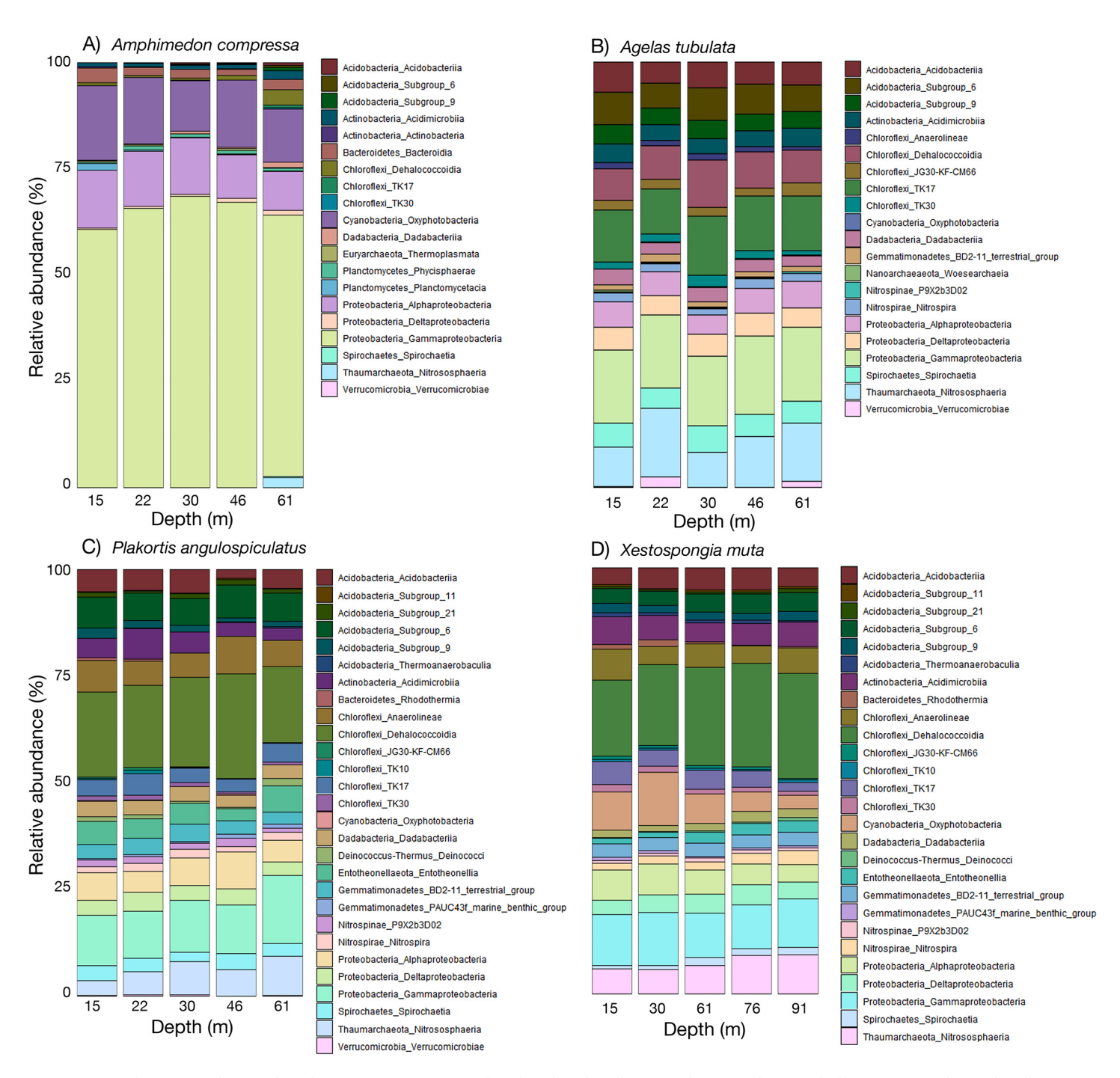


Fig. 2. Average relative abundance (percentage) at the class level in the microbiomes along a shallow to mesophotic depth gradient from (A) Amphimedon compressa, (B) Agelas tubulata, (C) Plakortis angulospiculatus and (D) Xestospongia muta

Seawater samples showed an effect of depth on microbial community composition at the class level (PERMANOVA: $F_{5,125} = 44.68$, p = 0.001) but not at the phylum level (Fig. S3). Generally, there were significant reductions in the percentage of ASVs for *Oxyphotobacteria*, *Bacteriodia*, *Gammaproteo-*

bacteria and Alphaproteobacteria with depth (Tukey's HSD < 0.05; Table S3), while there were significant increases in the Dehalococcidia, Thermoplasmata, Deltaproteobacteria, 'OM_190' (Phylum Planctomycetes) and Acidimicrobiia with depth (Tukey's HSD < 0.05; Table S3).

3.2. Predictive functional profiling of selected KEGG orthologs

The mean NSTI score, a metric of prediction accuracy, in PICRUSt2 (Langille et al. 2013) for the sampled sponges was 0.41 ± 0.09 and ranged from 0.03 to 0.53, where PICRUSt2 is set to a cut-off of 2.0 to prevent lower confidence predictions of function. For samples of A. compressa, genes for carbon metabolism (glycolysis and tricarboxcylic acid [TCA] cycle) and nitrogen metabolism (denitrification, nitrification and N-fixation) showed a significant decrease in relative abundance with increasing depth (Table S4). Genes involved in the Calvin Cycle and phosphate metabolism showed a significant increase in relative abundance with increasing depth (Table S4). For samples of A. tubulata, genes associated with carbon metabolism (glycolysis and TCA cycle) and nitrogen metabolism (denitrification, nitrification and N-fixation) showed a significant decrease in relative abundance with increasing depth (Table S5). Genes associated with the Calvin Cycle, photosynthesis and nitrogen metabolism (N-reduction) showed a significant increase in relative abundance with increasing depth (Table S5). In samples from P. angulospiculatus, genes associated with glycolysis, TCA cycle, glyoxylate cycle, N-fixation and N-reduction showed a significant decrease in relative abundance with increasing depth (Table S6). Genes associated with the Calvin Cycle, regulation of N-fixation and nitrification showed a significant increase in relative abundance with increasing depth (Table S6). In samples from X. muta, genes associated with the carbon cycle (Calvin Cycle and photosynthesis) and the nitrogen cycle (Nreduction) showed a significant decrease in relative

abundance with increasing depth (Table S7). Genes associated with the TCA cycle, N-fixation regulation and denitrification showed a significant increase in relative abundance with increasing depth (Table S7).

3.3. Stable isotope analyses

Using small sample size-corrected standard ellipse areas (SEAc) in SIBER, an assessment of isotopic niche space was generated for the sponges collected in this study as a function of species and depth. The HMA sponges P. angulospiculatus and X. muta grouped separately from each other, while the HMA sponge A. tubulata grouped with the LMA sponge A. compressa (Fig. 3, Table S8). Additionally, trophic niche separation (i.e. autotrophic, mixotrophic, heterotrophic) occurred as a function of depth in all sponges assessed, including A. compressa (Fig. S4). There was a significant effect of depth on δ^{13} C in *P. angu*lospiculatus ($t_{28} = -2.88$, p = 0.007), which decreased with increasing depth (Fig. 4, Table S9). There were no significant effects of depth on the δ^{13} C of *A. tubu*lata ($t_{23} = -1.40$, p = 0.174), A. compressa ($t_{17} = 0.972$, p = 0.338) or *X. muta* ($t_{21} = 0.99$, p = 0.334). There was a significant effect of depth on $\delta^{15}N$ in A. compressa $(t_{17} = 2.21, p = 0.042), P. angulospiculatus (t_{28} = 3.93, p = 0.042),$ p = 0.02) and X. muta ($t_{28} = 3.12$, p = 0.002), which increased with increasing depth (Fig. 4, Table S9). There was no significant effect of depth on δ^{15} N in A. tubulata ($t_{23} = 1.78$, p = 0.06), but a trend of increasing $\delta^{15}N$ with increasing depth was observed. There was a significant effect of depth on the C:N ratios of A. tubulata ($t_{23} = 3.08$, p = 0.005), which increased with increasing depth (Table S9). There were no sig-

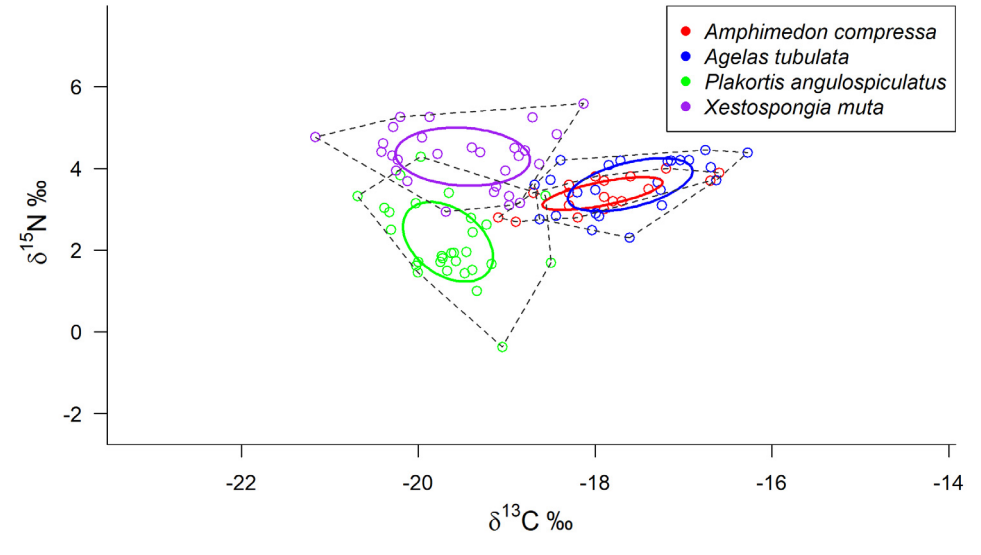


Fig. 3. Trophic niche separation between Amphimedon compressa, Agelas tubulata, Plakortis angulospiculatus and Xestospongia muta. Ellipses were calculated in SIBER using SEAc values and represent the isotopic niche of each species from all depths

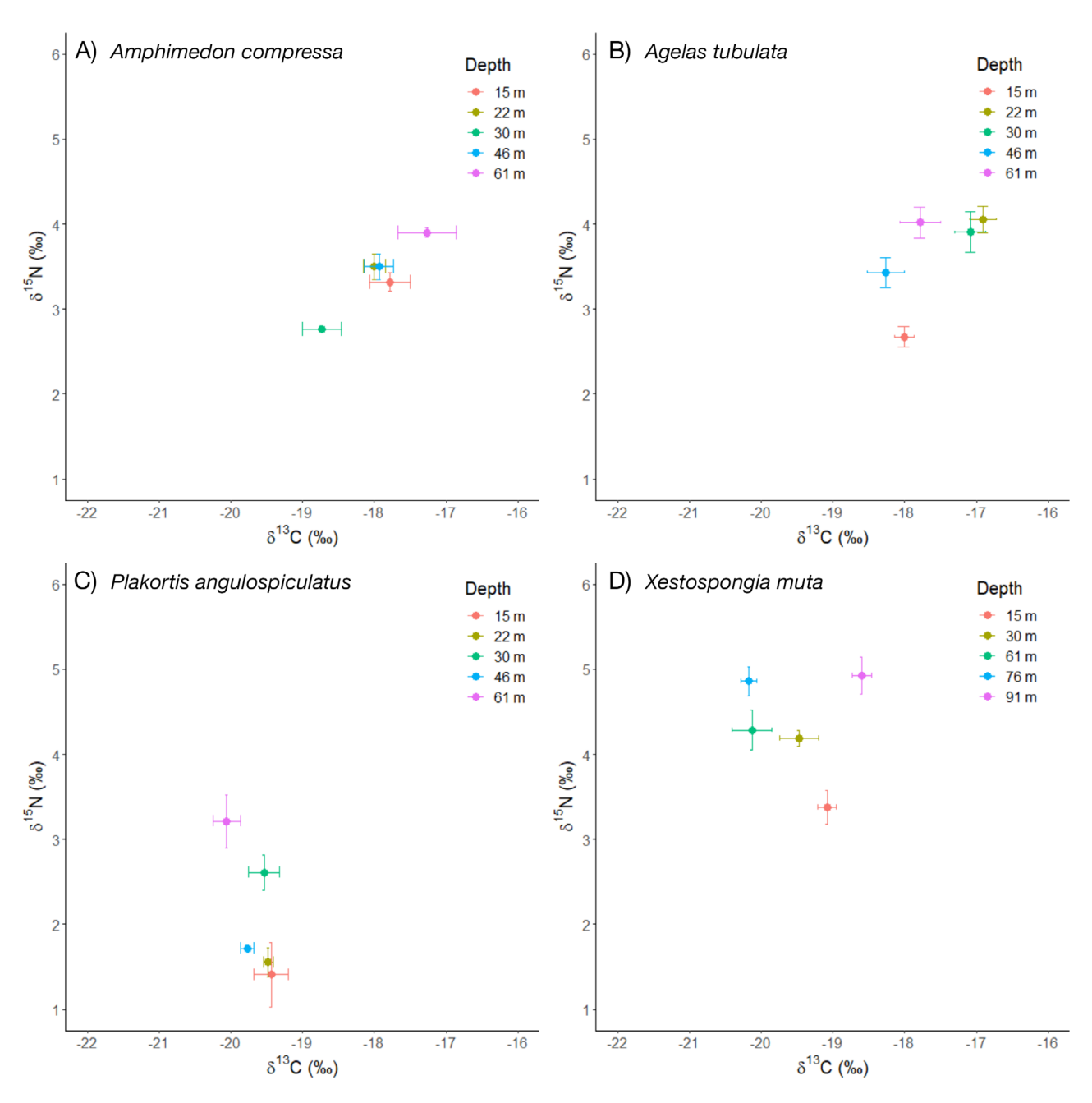


Fig. 4. Bivariate plots of mean (\pm SE) δ^{13} C and δ^{15} N between depths for (A) Amphimedon compressa, (B) Agelas tubulata, (C) Plakortis angulospiculatus and (D) Xestospongia muta

nificant effects of depth on the C:N ratios of *A. compressa* ($t_{17} = 0.007$, p = 0.933), *P. angulospiculatus* ($t_{28} = 1.43$, p = 0.164) or *X. muta* ($t_{21} = 0.25$, p = 0.803; Table S9).

3.4. Proximate biochemical composition

For *A. compressa*, as depth increased, carbohydrates and soluble protein increased ($t_{21} = 4.42$, p = 0.0003;

 $t_{21}=3.25$, p = 0.004, respectively), while lipids decreased ($t_{21}=-4.84$, p < 0.0001). However, there was no significant effect of depth on total energetic content ($t_{21}=-1.26$, p = 0.22). For *A. tubulata*, as depth increased, carbohydrates and soluble protein concentrations increased ($t_{29}=4.29$, p = 0.0002; $t_{29}=3.40$, p = 0.0021, respectively), while lipids and total energetic content decreased ($t_{29}=-6.45$, p < 0.0001; $t_{29}=-2.23$, p = 0.034, respectively; Table S10). In *P. angulospiculatus*, there were no significant effects of depth on the

concentration of carbohydrates, soluble protein, lipids or total energetic content ($t_{29}=0.91$, p=0.375; $t_{29}=-0.11$, p=0.911; $t_{29}=-0.64$ p=0.526; $t_{29}=1.96$, p=0.062, respectively). For *X. muta*, as depth increased, carbohydrates, soluble protein and total energetic content concentrations increased ($t_{29}=7.11$, p=0.0001; $t_{29}=3.63$, p=0.0013; $t_{29}=3.72$, p=0.0011, respectively), while lipid concentrations decreased ($t_{29}=-3.05$, p<0.0055; Table S10).

4. DISCUSSION

4.1. Species-specific shifts in microbiome structure and function between depths

The sponges sampled in this study showed a similar pattern of species-specific microbial communities previously reported for many sponge species (Thomas et al. 2016, Pita et al. 2018). While HMA sponges share many of the same phyla (Thomas et al. 2016, Pita et al. 2018), the relative abundance of each varies for each sponge species. This suggests that these microbial phyla play important roles in sponges but that their contributions to the trophic and chemical ecology probably vary between host species.

Of the 4 sponge species sampled, only the community structure of the Agelas tubulata microbiome did not change with depth, but there were significant differences due to depth in the predicted functions (i.e. functional capacity) of the A. tubulata microbiome. Changes in nitrogen and carbon cycling with depth did occur in A. tubulata, which suggests that the microbiome may alter its functional capacity for different pathways in response to changes in the environment, or the quantity and quality of POM and DOM, with depth. The microbiome of A. tubulata has a significant population of microbes from the phyla Proteobacteria and Chloroflexi, which have been shown to have high physiological diversity (Bayer et al. 2018, Pita et al. 2018, Fiore et al. 2020). However, Amphimedon compressa, Xestospongia muta and Plakortis angulospiculatus did show significant, or species-specific, changes in their microbiomes with depth. These changes in microbiome composition and function could be driven by changes in the availability of trophic resources, but while DOC does decrease with depth, as does its proportion of recalcitrant to labile components (Wagner et al. 2020), it is highly unlikely that the sponge holobiont is carbonlimited at any depth (Lesser et al. 2018). Decreases in DON with concurrent increases in NO_x with depth (Macartney et al. 2021b) may also cause changes in

microbiome composition given the importance of nitrogen in cell growth and that NO₃⁻ and NO₂⁻ are important components in the nitrogen budget of heterotrophic microbes (Horrigan et al. 1988). The observed increase in NO_x with increasing depth at this site (Macartney et al. 2021b) could result in changes in the trophic strategy and community composition of both bacterioplankton and the sponge microbiome. Additionally, the increased consumption of higher quality, low C:N ratio POM by sponges could cause changes in microbial metabolism. Changes in the functional metabolic capacity for the sponge microbiome, specifically in carbon and nitrogen metabolism, varied as a function of depth based on metagenomic profiling using PICRUSt2. These shifts in predicted microbiome function with depth may reflect species-specific trophic niche partitioning, as reported here based on the stable isotopic data, and for other locations in the Caribbean (e.g. Freeman et al. 2020).

4.2. HMA and LMA sponges rely more heavily on POM in the mesophotic zone

All sponge species in this study showed a pattern of increasing δ^{15} N as depth increased (Fig. 4, Table S9). This increase in $\delta^{15}N$ has also been observed at other sites in the Caribbean basin such as the Bahamas, Curacao and Little Cayman (Slattery et al. 2011, Morrow et al. 2016, Lesser et al. 2020, Macartney et al. 2021a,b) and reflects an increase in the consumption of POM—specifically heterotrophic picoplankton, which is more abundant as depth increases (Lesser 2006, Trussell et al. 2006, Lesser et al. 2019, 2020). This finding is also supported by the isotopic niche separation based on the SIBER SEAc analysis of stable isotopes between depths for each species (Fig. S4). The increased availability of POM at mesophotic depths is known to be associated with higher growth rates and abundances in Caribbean sponges as depth increases (Lesser 2006, Trussell et al. 2006, Slattery & Lesser 2015, Macartney et al. 2021b). Species differences in the trophic ecology of the sponges examined here occur as a function of increasing depth as well as differences based on HMA/LMA status (i.e. stable isotopic signatures), making it unlikely that the significant increase in $\delta^{15}N$ in all sponges is driven by changes in their microbiome community or function.

DOM on coral reefs decreases from shallow to mesophotic depths and has an increasingly greater C:N ratio (Lesser et al. 2019, 2020, Macartney et al. 2021b) due to the utilization of its labile, more nitro-

gen-rich components (Wagner et al. 2020). With DOM $\delta^{15}N$ signatures on coral reefs typically between 3 and 4% (Thibodeau et al. 2013) and the reduction in both quality (recalcitrant versus labile) and quantity of DOM (i.e. both DOC and DON), the most parsimonious explanation for the changes in $\delta^{15}N$ with depth is that these sponges consume more POM as depth increases into the mesophotic, and the $\delta^{15}N$ signature becomes enriched as a result of fractionation processes associated with the increased feeding on POM (Fry 2006).

4.3. Variation in $\delta^{13}C$ and $\delta^{15}N$ between sponge species

All of the sponges in this study show a general increase in $\delta^{15}N$ as depth increases. This suggests an increased consumption, in proportion to its abundance, of low C:N heterotrophic picoplankton into the mesophotic zone (Macartney et al. (2021 a). For P. angulospiculatus, lower $\delta^{15}N$ values were observed in samples from 15 to 30 m, which could reflect inputs of nitrogen produced via N-fixation pathways (N-fixation $\delta^{15}N\!\!:\!-2$ to 2%). The potential for N-fixation has been previously reported in sponges (Mohamed et al. 2008), where N-fixation could occur during decreased, or cessation of, pumping, resulting in hypoxic tissue compartments that would facilitate N-fixation by the enzyme nitrogenase, a uniquely prokaryotic and oxygen-sensitive enzyme (Mohamed et al. 2008, Fiore et al. 2010). In this study it was observed that P. angulospiculatus contained small relative abundances (<5%) of cyanobacteria, a taxon known to fix nitrogen. These sponges, however, are also exposed to higher concentrations of DON at shallow depths which might repress nitrogenase activity. Alternatively, assuming that P. angulospiculatus is not preferentially feeding on more diazotrophs from the plankton compared to other sponge species, another explanation for the low $\delta^{15}N$ sponge tissue values may be the result of other microbial transformations in the nitrogen cycle such as nitrification (Southwell et al. 2008).

The δ^{13} C in the tissues of both *X. muta* and *P. angulospiculatus* suggests that photoautotrophic carbon inputs to the sponge's carbon budget are occurring (Fry 2006, Slattery et al. 2011). These signals could be derived from translocation of photosynthates from symbionts to host tissues (Morrow et al. 2016, Gantt et al. 2019), or from the DOM of either macrophytes or corals with a δ^{13} C of DOM of –11.21 to –19.50% for macrophytes (van Duyl et al. 2018) and –15.46 to

-17.95% (van Duyl et al. 2011) for corals. For X. muta, there was a trend of decreasing abundance of cyanobacteria with depth corresponding to decreases in the genes associated with photosynthesis. In P. angulospiculatus, however, much smaller abundances of cyanobacteria are present, so the $\delta^{13}C$ of both sponges could reflect the trophic resources available to them (POM and DOM) and subsequent carbon cycling within their microbiome. While there were large communities of Chloroflexi in all the HMA sponges examined here, there is no signal of autotrophy by anaerobic carbon fixation pathways in the δ^{13} C (~-14.0%) of *X. muta* and *P. angulospicula*tus (Canfield et al. 2005). The δ^{13} C of both A. compressa and A. tubulata, both HMA sponges, were ~2% higher (-17 to -18%) compared to X. muta and *P. angulospiculatus*, which overlaps with the δ^{13} C of marine POM which has been shown to range from −16.0 to −18.0‰ on more inshore, or coastal, coral reefs where detritus is a significant component (Lamb & Swart 2008) similar to where sponges in this study were collected. For both A. compressa and A. tubulata these values also become increasingly lighter as depth increases, suggesting increasing dependence on POM which is more bioavailable for consumption than DOM (Lønborg et al. 2018).

4.4. Shared isotopic niche space by an LMA and HMA sponge

The HMA/LMA dichotomy is generally believed to influence the feeding strategy of a sponge (Weisz et al. 2008, Morganti et al. 2017). Typically, LMA sponges have higher pumping rates and increased consumption of POM. Conversely, HMA sponges typically have lower pumping rates and increased consumption of DOM (Weisz et al. 2008, Poppell et al. 2014). One confounding issue is the influence of sponge size on pumping rates (Lesser 2006). A detailed study by Morganti et al. (2019) showed that both HMA/LMA status and sponge size influence pumping and subsequently feeding rates. In this study, A. tubulata and A. compressa share a similar isotopic niche, so regardless of their HMA or LMA status, both appear to rely more heavily on POM for growth based on their tissue δ^{13} C values. Supporting this, samples of A. tubulata are reported to have lower ΣV values, a metric for microbial resynthesis and translocation of amino acids, compared to X. muta and P. angulospiculatus as described in Macartney et al. (2021a). This suggests that A. tubulata does not rely heavily on resynthesized and translocated amino acids from its microbiome relative to the other HMA sponges studied.

All 4 sponge species studied here can be defined as mixotrophs. But A. tubulata and A. compressa exhibit significant overlap in their isotopic niche space despite the fact they are defined as an HMA and LMA sponge, respectively. However, A. tubulata could be further defined as an HMA-L sponge which contains low concentrations of chorophyll (sensu van Duyl et al. 2018) and often overlaps in isotopic niche space with LMA sponges as observed here with A. compressa. Given this, the most parsimonious interpretation of the bulk tissue δ^{13} C data, and the isotopic niche space analysis, for A. tubulata and A. compressa, is that these species rely more on POM as a carbon source, despite their respective designations as HMA and LMA sponges. They also rely primarily on POM as a source of nitrogen, as their $\delta^{15}N$ values are similar and overlap based on the SIBER analysis. These results can then be compared to X. muta, and P. angulospiculatus which depend more on DOM or photoautotrophy as a source of carbon. and are clearly separated from A. tubulata and A. compressa in isotopic niche space. This is further complicated by studies showing that DOM (i.e. specifically DOC) can constitute up to 90% of an LMA sponge's carbon budget but POM remains a major source of nitrogen (Morganti et al. 2017, Bart et al. 2020). Additionally, the proportion of DOM that is taken up by the microbiome compared to the host in an HMA sponge ranges from 65 to 87%, while in an LMA sponge it is <5% (e.g. Rix et al. 2020). To reduce ambiguity on the trophic ecology of the HMA/ LMA dichotomy, additional experimental studies including compound-specific isotopic approaches (e.g. Macartney et al. 2021a) or a combination of bulk stable isotopes, tracer studies, NanoSIMS and tissue fractionation (e.g. Achlatis et al. 2019) should be undertaken.

4.5. Increased mesophotic POM availability results in phenotypic plasticity in energetic strategies

The PBC of *A. compressa*, *A. tubulata* and *X. muta* showed significant differences as a function of increasing depth, with lipids decreasing and carbohydrates and soluble protein increasing at mesophotic depths. Most nutrient-sufficient marine invertebrates exposed to increased food resources, such as POM for mesophotic sponges, commonly increase their lipid reserves (Sokolova 2013). Lipid stores are then available for mobilization during periods of food lim-

itation, reproduction or seasonal growth. It seems unlikely that sponges at mesophotic depths are under stress or food-limitation conditions, as they are feeding on both POM and DOM at higher rates than their shallow conspecifics (Macartney et al. 2021b) and are generally buffered from potential abiotic stressors (Lesser et al. 2009). Based on this, it appears that the mesophotic sponges in this study prioritize growth over energetic reserves as proteins increase while lipids decrease with depth.

Sponges are known to exhibit phenotypic plasticity in chemical defenses, metabolic rate, morphology and spicule size (Bavestrello et al. 1993, Hill & Hill 2002, Morley et al. 2016, Slattery et al. 2016). It is also possible that sponges exhibit phenotypic plasticity in their energetic state, as seen in other marine invertebrates (Padilla & Savedo 2013). One such study, Slattery et al. (2016), found that P. angulospiculatus has plasticity in its ability to regenerate tissue versus chemical defenses between mesophotic and shallow depths, with mesophotic sponges prioritizing regeneration (e.g. protein synthesis) over chemical defense production, despite higher bite scar densities on mesophotic sponges. This effect was due to higher POM availability at deep sites. Since increased sponge growth rates are associated with increased picoplankton availability, with their more balanced C:N ratio, and consumption (Lesser 2006, Trussell et al. 2006, Lesser et al. 2018, 2019, 2020, Macartney et al. 2021b), an increase in the mobilization of macromolecules, such as lipids, with high energetic content for wound regeneration is then plausible for mesophotic sponges. The pattern of decreasing lipid concentration with depth was observed for the HMA sponges A. tubulata and X. muta and the LMA sponge A. compressa. As emergent LMA sponges typically utilize POM as a source of nitrogen in their diet compared to DOM (Morganti et al. 2017, McMurray et al. 2018, van Duyl et al. 2018), this suggests that POM availability is a proximate cause for the observed changes in the PBC of this species.

An alternate explanation is that the sponges on shallow reefs are exposed to more cyanobacteria, which have higher lipid content relative to other heterotrophic bacterioplankton (Fernandes da Silva et al. 2008, Karatay & Dönmez 2011), while sponges in the mesophotic are exposed to bacterioplankton populations with significantly fewer cyanobacteria (Lesser 2006, Trussell et al. 2006, Lesser et al. 2019, 2020). The observed differences in PBC are likely caused by both plasticity in energetic strategy and shifts in the types of picoplankton as depth changes. The contributions from heterotrophic symbionts to

sponge energetic budgets remain largely unquantified (Rix et al. 2020), leaving a large gap in our understanding of the contributions of DOM to sponge energetics. It is also possible that the concentrations of lipids are a reflection of the PBC of the microbiome of these sponges. However, the lipid concentration of bacteria is low (0.5–2.0 mg g⁻¹ dry weight) (Gillan et al. 1988, Fernandes da Silva et al. 2008) relative to the values for the sponge holobionts, and most of the variability in the biochemical composition we see in this study reflects the sponge host tissue and not its microbiome.

5. CONCLUSIONS

In this study, sponges across the shallow to mesophotic depth gradient showed species-specific patterns in microbial community structure, with microbiomes that undergo significant compositional changes as a function of depth regardless of HMA or LMA status. These species-specific microbiomes have complex carbon and nitrogen cycling capacities that also change along the depth gradient. These patterns are, again, species-specific, and the gradients in POM, PAR, DOM and NO_x are likely factors affecting these compositional and functional changes, highlighting the importance of collecting environmental data when assessing sponge microbiome community structure and function along environmental gradients (e.g. Lesser et al. 2009, 2019, Macartney et al. 2021a,b). The increased POM and the composition of that POM on MCEs appears to be reflected in both the $\delta^{15}N$ and PBC signatures of sponge tissue, which relates to phenotypic plasticity in their trophic ecology and energetic state between shallow and mesophotic depths. It is likely that sponges prioritize growth over energetic reserves in the mesophotic due to increased POM availability. Gradients in abiotic factors can change sponge microbial communities and their function at a local scale, but broad generalizations regarding sponge biogeochemical cycling, trophic strategy and energetics should be approached carefully given the species-specific variability observed in this study. While speciesspecific patterns in microbial community structure and function were observed in this study, all the sponges in this study consumed more heterotrophic picoplankton as depth increased based on stable isotope analysis, providing increased evidence that sponge distributions.

Acknowledgements. We thank E. Kintzing, A. Chavez and D. Gochfeld for field and laboratory support. We thank A. Weinheimer for assistance and advice on statistical analyses of 16s rRNA metabarcoding data. All sample collections complied with the laws of the Cayman Islands and the USA. Support was provided by NSF Biological Oceanography (OCE–1632348/1632333) to M.P.L. and M.S. respectively, and the University of New Hampshire Marine Biology Small Grants fund to K.J.M. The manuscript was partially based on a doctoral dissertation by K.J.M. at the University of New Hampshire.

LITERATURE CITED

- Abraham AC, Gochfeld DJ, Macartney KJ, Mellor A, Lesser MP, Slattery M (2021) Biochemical variability in sponges across the Caribbean basin. Invertebr Biol 140: e12341
- Achlatis M, Pernice M, Green K, de Goeij JM and others (2019) Single-cell visualization indicates direct role of sponge host in uptake of dissolved organic matter. Proc R Soc B 286:20192153
- Apprill A, McNally S, Parsons R, Weber L (2015) Minor revision to V4 region SSU rRNA 806R gene primer greatly increases detection of SAR11 bacterioplankton. Aquat Microb Ecol 75:129–137
- Barbera P, Kozlov AM, Czech L, Morel B, Darriba D, Flouri T, Stamatakis A (2019) EPA-ng: massively parallel evolutionary placement of genetic sequences. Syst Biol 68: 365–369
- ▶ Bart MC, de Kluijver A, Hoetjes S, Absalah S and others (2020) Differential processing of dissolved and particulate organic matter by deep-sea sponges and their microbial symbionts. Sci Rep 10:17515
 - Bavestrello G, Bonito M, Sarà M (1993) Influence of depth on the size of sponge spicules. Sci Mar 57:415–420
- Bayer K, Jahn MT, Slaby BM, Moitinho-Silva L, Hentschel U (2018) Marine sponges as *Chloroflexi* hot spots: genomic insights and high-resolution visualization of an abundant and diverse symbiotic clade. mSystems 3:e00150-18
- ≈ Bell JJ (2008) The functional roles of marine sponges. Estuar Coast Shelf Sci 79:341–353
- Bongaerts P, Ridgway T, Sampayo EM, Hoegh-Guldberg O (2010) Assessing the 'deep reef refugia' hypothesis: focus on Caribbean reefs. Coral Reefs 29:309–327
- Bongaerts P, Riginos C, Brunner R, Englebert N, Smith SR, Hoegh-Guldberg O (2017) Deep reefs are not universal refuges: reseeding potential varies among coral species. Sci Adv 3:e1602373
- Bourne DG, Morrow KM, Webster NS (2016) Insights into the coral microbiome: underpinning the health and resilience of reef ecosystems. Annu Rev Microbiol 70:317–340
- ▶ Bradford MM (1976) A rapid and sensitive method for the quantitation of microgram quantities of protein utilizing the principle of protein-dye binding. Anal Biochem 72: 248–254
- Callahan BJ, Sankaran K, Fukuyama JA, McMurdie PJ, Holmes SP (2016) Bioconductor workflow for microbiome data analysis: from raw reads to community analyses. F1000 Res 5:1492
- Campbell L, Nolla HA, Vaulot D (1994) The importance of Prochlorococcus to community structure in the central North Pacific Ocean. Limnol Oceanogr 39:954–961
- bottom-up processes play a significant role in Canfield DE, Kristensen E, Thamdrup B (2005) Carbon fixasponge distributions tion and phototrophy. Adv Mar Biol 48:95–127

- **de Goeij JM, van Oevelen D, Vermeij MJ, Osinga R, Middelburg JJ, De Goeij AF, Admiraal W (2013) Surviving in a marine desert: the sponge loop retains resources within coral reefs. Science 342:108–110
 - de Goeij JM, Lesser MP, Pawlik JR (2017) Nutrient fluxes and ecological functions of coral reef sponges in a changing ocean. In: Carballo J, Bell J (eds) Climate change, ocean acidification and sponges. Springer International, Cham, p 373–410
 - Diamond JM (1986) Overview: laboratory experiments, field experiments and natural experiments. In: Diamond JM, Case TJ (eds) Community ecology. Harper & Row, New York, NY, p 3–22
 - Diaz MC, Rützler K (2001) Sponges: an essential component of Caribbean coral reefs. Bull Mar Sci 69:535–546
- Ducklow HW, Kirchman DL, Quinby HL, Carlson CA, Dam HG (1993) Stocks and dynamics of bacterioplankton carbon during the spring bloom in the eastern North Atlantic Ocean. Deep Sea Res II 40:245–263
- Duhamel S, van Wambeke V, Lefevre D, Benavides M, Bonnet S (2018) Mixotrophic metabolism by natural communities of unicellular cyanobacteria in the western tropical South Pacific Ocean. Environ Microbiol 20:2743–2756
- Eddy SR (2008) A probabilistic model of local sequence alignment that simplifies statistical significance estimation. PLOS Comput Biol 4:e1000069
- Fernandes da Silva C, Ballester E, Monserrat J, Geracitano L, Wasielesky W Jr, Abreu PC (2008) Contribution of microorganisms to the biofilm nutritional quality: protein and lipid contents. Aquacult Nutr 14:507–514
- Fiore CL, Jarett JK, Olson ND, Lesser MP (2010) Nitrogen fixation and nitrogen transformations in marine symbioses. Trends Microbiol 18:455–463
- Fiore CL, Baker DM, Lesser MP (2013a) Nitrogen biogeochemistry in the Caribbean sponge, *Xestospongia muta*: A source or sink of dissolved inorganic nitrogen? PLOS ONE 8:e72961
- Fiore CL, Jarett JK, Lesser MP (2013b) Symbiotic prokaryotic communities from different populations of the giant barrel sponge, *Xestospongia muta*. MicrobiologyOpen 2: 938–952
- Fiore CL, Labrie M, Jarett JK, Lesser MP (2015) Transcriptional activity of the giant barrel sponge, *Xestospongia muta* holobiont: molecular evidence for metabolic interchange. Front Microbiol 6:364
- Fiore CL, Jarett JK, Steinert G, Lesser MP (2020) Trait-based comparison of coral and sponge microbiomes. Sci Rep 10:1–6
- Freeman CJ, Easson CG, Matterson KO, Thacker RW, Baker DM, Paul VJ (2020) Microbial symbionts and ecological divergence of Caribbean sponges: a new perspective on an ancient association. ISME J 14:1571–1583
 - Freeman NK, Lindgren FT, Ng YO, Nichols AV (1957) Infrared spectra of some lipoproteins and related lipids. J Biol Chem 203:293–304
- Fry B (2006) Stable isotope ecology. Springer, New York, NY Gantt SE, McMurray SE, Stubler AD, Finelli CM, Pawlik JR, Erwin PM (2019) Testing the relationship between microbiome composition and flux of carbon and nutrients in Caribbean coral reef sponges. Microbiome 7:124
- Garcia-Sais JR (2010) Reef habitats and associated sessilebenthic and fish assemblages across a euphoticmesophotic depth gradient in Isla Desecheo, Puerto Rico. Coral Reefs 29:277–288
- 🏋 Gillan FT, Stoilov IL, Thompson JE, Hogg RW, Wilkinson

- CR, Djerassi C (1988) Fatty acids as biological markers for bacterial symbionts in sponges. Lipids 23:1139–1145
- Gloeckner V, Wehrl M, Moitinho-Silva L, Gernert C, Schupp P, Pawlik JR, Hentschel U (2014) The HMA-LMA dichotomy revisited: an electron microscopical survey of 56 sponge species. Biol Bull (Woods Hole) 227:78–88
- Gnaiger E, Bitterlich G (1984) Proximate biochemical composition and caloric content calculated from elemental CHN analysis: a stoichiometric concept. Oecologia 62: 289–298
- Hentschel U, Usher KM, Taylor MW (2006) Marine sponges as microbial fermenters. FEMS Microbiol Ecol 55:167–177
- Hentschel U, Piel J, Degnan SM, Taylor MW (2012) Genomic insights into the marine sponge microbiome. Nat Rev Microbiol 10:641–654
- Hill MS, Hill AL (2002) Morphological plasticity in the tropical sponge *Anthosigmella varians*: responses to predators and wave energy. Biol Bull (Woods Hole) 202:86–95
- *Horrigan SG, Hagström Å, Koike I, Azam F (1988) Inorganic nitrogen utilization by assemblages of marine bacteria in seawater culture. Mar Ecol Prog Ser 50:147–150
- Hudspith M, Rix L, Achlatis M, Bougoure J and others (2021) Subcellular view of host-microbiome nutrient exchange in sponges: insights into the ecological success of an early metazoan-microbe symbiosis. Microbiome 9:44
- Jackson AL, Inger R, Parnell AC, Bearhop S (2011) Comparing isotopic niche widths among and within communities: SIBER–Stable Isotope Bayesian Ellipses in R. J Anim Ecol 80:595–602
- Karatay SE, Dönmez G (2011) Microbial oil production from thermophile cyanobacteria for biodiesel production. Appl Energy 88:3632–3635
- Lamb K, Swart PK (2008) The carbon and nitrogen isotopic values of particulate organic material from the Florida Keys: a temporal and spatial study. Coral Reefs 27:351–362
- Langille MGI (2018) Exploring linkages between taxonomic and functional profiles of the human microbiome. mSystems 3:e00163-17
- Langille MGI, Zaneveld J, Caporaso JG, McDonald D and others (2013) Predictive functional profiling of microbial communities using 16S rRNA marker gene sequences.

 Nat Biotechnol 31:814–821
- Layman CA, Arrington DA, Montaña CG, Post DM (2007)
 Can stable isotope ratios provide for community-wide measures of trophic structure? Ecology 88:42–48
- Lesser MP (2006) Benthic-pelagic coupling on coral reefs: feeding and growth of Caribbean sponges. J Exp Mar Biol Ecol 328:277–288
- Lesser MP, Slattery M (2013) Ecology of Caribbean sponges: Are top-down or bottom-up processes more important? PLOS ONE 8:e79799
- Lesser MP, Slattery M (2018) Sponge density increases with depth throughout the Caribbean. Ecosphere 9:e02525
- Lesser MP, Slattery M, Leichter JJ (2009) Ecology of mesophotic coral reefs. J Exp Mar Biol Ecol 375:1–8
- **Lesser MP, Slattery M, Mobley CD (2018) Biodiversity and functional ecology of mesophotic coral reefs. Annu Rev Ecol Syst 49:49–71
- Lesser MP, Slattery M, Laverick JH, Macartney KJ, Bridge TC (2019) Global community breaks at 61 m on mesophotic coral reefs. Glob Ecol Biogeogr 28:1403–1416
- Lesser MP, Mueller B, Pankey MS, Macartney KJ, Slattery M, de Goeij JM (2020) Depth-dependent detritus production in the sponge, *Halisarca caerulea*. Limnol Oceanogr 65:1200–1216

- Lesser MP, Mobley CD, Hedley JD, Slattery M (2021) Incident light on mesophotic corals is constrained by reef topography and colony morphology. Mar Ecol Prog Ser 670: 49–60
- Leys SP, Kahn AS, Fang JK, Kutti T, Bannister RJ (2018) Phagocytosis of microbial symbionts balances the carbon and nitrogen budget for the deep-water boreal sponge *Geodia barretti*. Limnol Oceanogr 63:187–202
- Lønborg C, Álvarez-Salgado XA, Duggan S, Carreira C (2018) Organic matter bioavailability in tropical coastal waters: The Great Barrier Reef. Limnol Oceanogr 63: 1015–1035
- Loya Y, Eyal G, Treibitz T, Lesser MP, Appeldoorn R (2016)
 Theme section on mesophotic coral ecosystems: advances in knowledge and future perspectives. Coral Reefs 35:1–9
- Macartney KJ, Pankey MS, Slattery M, Lesser MP (2020) Trophodynamics of the sclerosponge *Ceratoporella nicholsoni* along a shallow to mesophotic depth gradient. Coral Reefs 39:1829–1839
- Macartney KJ, Slattery M, Lesser MP (2021a) Trophic ecology of Caribbean sponges in the mesophotic zone. Limnol Oceanogr 66:1113–1124
- Macartney KJ, Clayshulte Abraham A, Slattery M, Lesser MP (2021b) Growth and feeding in the sponge, *Agelas tubulata*, from shallow to mesophotic depths on Grand Cayman Island. Ecosphere 12:e03764
- Masuko T, Minami A, Iwasaki N, Majima T, Nishimura SI, Lee YC (2005) Carbohydrate analysis by a phenol–sulfuric acid method in microplate format. Anal Biochem 339:69–72
- McClintock J, Heine J, Slattery M, Weston J (1991) Biochemical and energetic composition, population biology, and chemical defense of the Antarctic ascidian *Cnemidocarpa* verrucosa Lesson. J Exp Mar Biol Ecol 147:163–175
- McMurdie PJ, Holmes S (2015) Shiny-phyloseq: web application for interactive microbiome analysis with provenance tracking. Bioinformatics 31:282–283
- McMurray SE, Stubler AD, Erwin PM, Finelli CM, Pawlik JR (2018) A test of the sponge-loop hypothesis for emergent Caribbean reef sponges. Mar Ecol Prog Ser 588:1–14
- Mohamed NM, Colman AS, Tal Y, Hill RT (2008) Diversity and expression of nitrogen fixation genes in bacterial symbionts of marine sponges. Environ Microbiol 10: 2910–2921
- Morganti T, Coma R, Yahel G, Ribes M (2017) Trophic niche separation that facilitates co-existence of high and low microbial abundance sponges is revealed by *in situ* study of carbon and nitrogen fluxes. Limnol Oceanogr 62: 1963–1983
- Morganti TM, Ribes M, Yahel G, Coma R (2019) Size is the major determinant of pumping rates in marine sponges. Front Physiol 10:1474
- Morley SA, Berman J, Barnes DK, de Juan Carbonell C, Downey RV, Peck LS (2016) Extreme phenotypic plasticity in metabolic physiology of Antarctic demosponges. Front Ecol Evol 33:157
- Morrow KM, Fiore CL, Lesser MP (2016) Environmental drivers of microbial community shifts in the giant barrel sponge, *Xestospongia muta*, over a shallow to mesophotic depth gradient. Environ Microbiol 18:2025–2038
- Mueller B, de Goeij JM, Vermeij MJ, Mulders Y, van der Ent E, Ribes M, van Duyl FC (2014) Natural diet of coralexcavating sponges consists mainly of dissolved organic carbon (DOC). PLOS ONE 9:e90152
- Olinger LK, Strangman WK, McMurray SE, Pawlik JR (2021) Sponges with microbial symbionts transform dissolved

- organic matter and take up organohalides. Front Mar Sci 8.548
- Olson JB, Gao X (2013) Characterizing the bacterial associates of three Caribbean sponges along a gradient from shallow to mesophotic depths. FEMS Microbiol Ecol 85: 74–84
- Padilla DK, Savedo MM (2013) A systematic review of phenotypic plasticity in marine invertebrate and plant systems. Adv Mar Biol 65:67–94
- Parada AE, Needham DM, Fuhrman JA (2016) Every base matters: assessing small subunit rRNA primers for marine microbiomes with mock communities, time series and global field samples. Environ Microbiol 18:1403–1414
- Pawlik JR, Loh TL, McMurray SE, Finell CM (2013) Sponge communities on Caribbean coral reefs are structured by factors that are top-down, not bottom-up. PLOS ONE 8: e62573
- Pawlik JR, McMurray SE, Erwin P, Zea S (2015) No evidence for food limitation of Caribbean reef sponges: Reply to Slattery & Lesser (2015). Mar Ecol Prog Ser 527: 281–284
- Pita L, Rix L, Slaby BM, Franke A, Hentschel U (2018) The sponge holobiont in a changing ocean: from microbes to ecosystems. Microbiome 6:46
- Poppell E, Weisz J, Spicer L, Massaro A, Hill A, Hill M (2014) Sponge heterotrophic capacity and bacterial community structure in high-and low-microbial abundance sponges. Mar Ecol 35:414–424
- Reiswig HM (1981) Partial carbon and energy budgets of the bacteriosponge *Verongia fistularis* (Porifera: Demospongiae) in Barbados. Mar Ecol 2:273–293
- Rix L, de Goeij JM, van Oevelen D, Struck U, Al-Horani FA, Wild C, Naumann MS (2017) Differential recycling of coral and algal dissolved organic matter via the sponge loop. Funct Ecol 31:778–789
- Rix L, Ribes M, Coma R, Jahn MT and others (2020) Heterotrophy in the earliest gut: a single-cell view of heterotrophic carbon and nitrogen assimilation in spongemicrobe symbioses. ISME J 14:2554–2567
- Rubin-Blum M, Antony CP, Sayavedra L, Martínez-Pérez C, Birgel D, Peckmann J, Sahling H (2019) Fueled by methane: deep-sea sponges from asphalt seeps gain their nutrition from methane-oxidizing symbionts. ISME J 13:1209–1225
- Schubert CJ, Nielsen B (2000) Effects of decarbonation treatments on δ¹³C values in marine sediments. Mar Chem 72:55–59
- Seutin G, White BN, Boag PT (1991) Preservation of avian blood and tissue samples for DNA analysis. Can J Zool 69:82-90
- Shih JL, Selph KE, Wall CB, Wallsgrove NJ, Lesser MP, Popp BN (2020) Trophic ecology of the tropical Pacific sponge *Mycale grandis* inferred from amino acid compound-specific isotopic analyses. Microb Ecol 79:495–510
- Slattery M, Lesser MP (2015) Trophic ecology of sponges from shallow to mesophotic depths (3 to 150 m): Comment on Pawlik et al. (2015). Mar Ecol Prog Ser 527: 275–279
- Slattery M, Lesser MP, Brazeau D, Stokes MD, Leichter JJ (2011) Connectivity and stability of mesophotic coral reefs. J Exp Mar Biol Ecol 408:32–41
- Slattery M, Gochfeld DJ, Diaz MC, Thacker RW, Lesser MP (2016) Variability in chemical defense across a shallow to mesophotic depth gradient in the Caribbean sponge Plakortis angulospiculatus. Coral Reefs 35:11–22

- Sokolova IM (2013) Energy-limited tolerance to stress as a conceptual framework to integrate the effects of multiple stressors. Integr Comp Biol 53:597–608
- Southwell MW, Popp BN, Martens CS (2008) Nitrification control on fluxes and isotopic composition of nitrate from Florida Keys sponges. Mar Chem 108:96–108
 - Steinert G, Taylor MW, Deines P, Simister RL, De Voogd NJ, Hoggard M, Schupp PJ (2016) In four shallow and mesophotic tropical reef sponges from Guam the microbial community largely depends on host identity. PeerJ 4:e1936
- Thacker RW, Freeman CJ (2012) Sponge–microbe symbioses.
 Recent advances and new directions. Adv Mar Biol 62:
 57–111
- Thibodeau B, Miyajima T, Tayasu I, Wyatt AS and others (2013) Heterogeneous dissolved organic nitrogen supply over a coral reef: first evidence from nitrogen stable isotope ratios. Coral Reefs 32:1103–1110
- Thomas T, Moitinho-Silva L, Lurgi M, Björk JR and others (2016) Diversity, structure and convergent evolution of the global sponge microbiome. Nat Commun 7:11870
- Trussell GC, Lesser MP, Patterson MR, Genovese SJ (2006)
 Depth-specific differences in growth of the reef sponge
 Callyspongia vaginalis: role of bottom-up effects. Mar
 Ecol Prog Ser 323:149–158
- Turner TF, Collyer ML, Krabbenhoft TJ (2010) A general hypothesis-testing framework for stable isotope ratios in ecological studies. Ecology 91:2227–2233
- xan Duyl FC, Moodley L, Nieuwland G, van Ijzerloo L and

Editorial responsibility: Pei-Yuan Qian, Kowloon, Hong Kong SAR Reviewed by: 3 anonymous referees

- others (2011) Coral cavity sponges depend on reefderived food resources: stable isotope and fatty acid constraints. Mar Biol 158:1653–1666
- wan Duyl FC, Mueller B, Meesters EG (2018) Spatio-temporal variation in stable isotope signatures (δ^{13} C and δ^{15} N) of sponges on the Saba Bank. PeerJ 6:e5460
- Wagner S, Schubotz F, Kaiser K, Hallmann C, Waska H, Rossel PE, Galy V (2020) Soothsaying DOM: a current perspective on the future of oceanic dissolved organic carbon. Front Mar Sci 7:341
- Weisz JB, Lindquist N, Martens CS (2008) Do associated microbial abundances impact marine demosponge pumping rates and tissue densities? Oecologia 155:367–376
- Wooster MK, McMurray SE, Pawlik JR, Morán XA, Berumen ML (2019) Feeding and respiration by giant barrel sponges across a gradient of food abundance in the Red Sea. Limnol Oceanogr 64:1790–1801
- Wulff J (2012) Ecological interactions and the distribution, abundance, and diversity of sponges. Adv Mar Biol 61: 273–344
- Wulff J (2017) Bottom-up and top-down controls on coral reef sponges: disentangling within-habitat and betweenhabitat processes. Ecology 98:1130–1139
- Ye Y, Doak TG (2009) A parsimony approach to biological pathway reconstruction/inference for genomes and metagenomes. PLOS Comput Biol 5:e1000465
- Zhang F, Jonas L, Lin H, Hill RT (2019) Microbially mediated nutrient cycles in marine sponges. FEMS Microbiol Ecol 95:fiz115

Submitted: July 12, 2021 Accepted: April 11, 2022

Proofs received from author(s): June 16, 2022